

Supplemental Figures

Figure S1

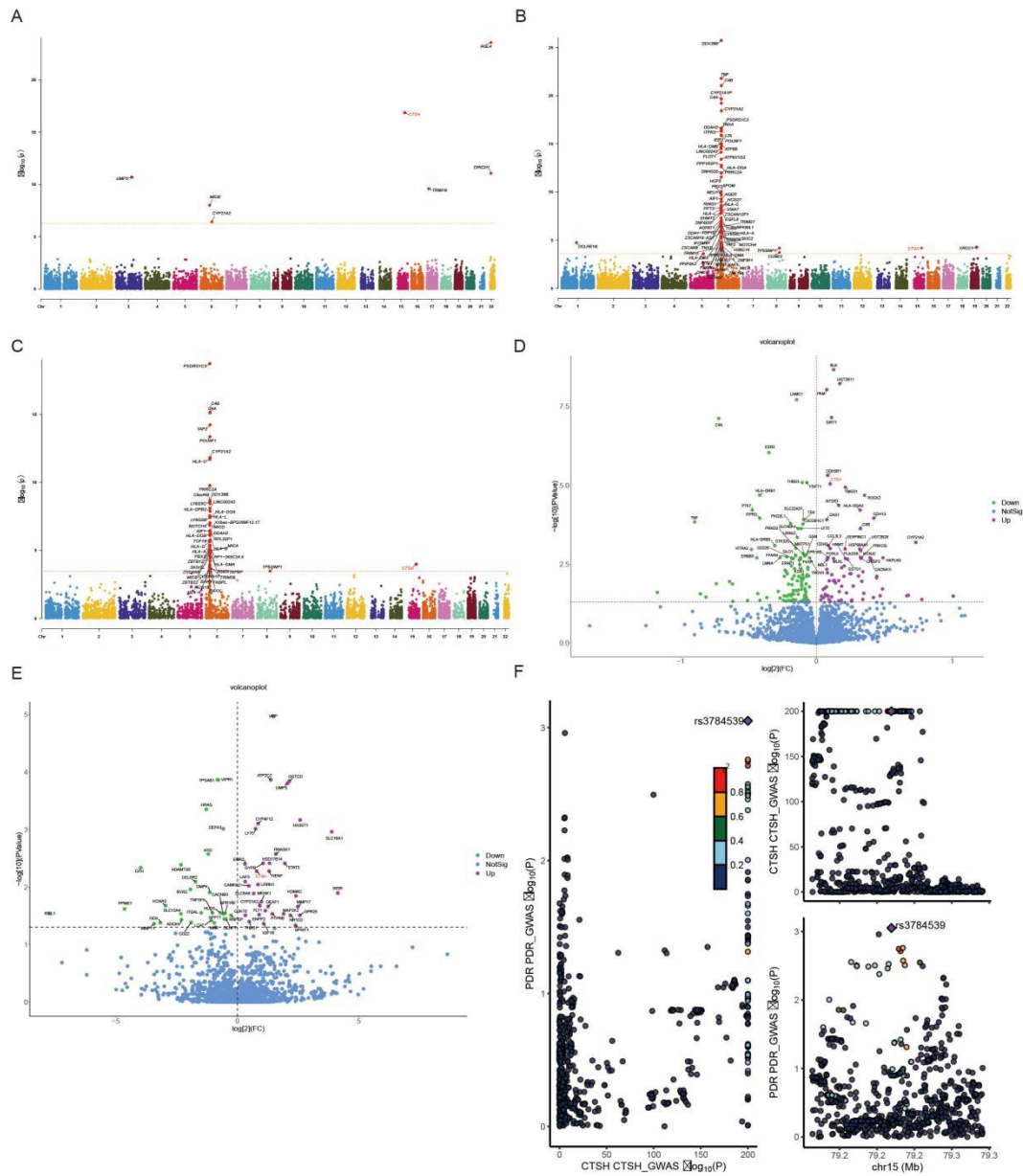


Figure S1. Genome-wide association and differential expression analyses

(A–C) Manhattan plots highlighting CTSH locus significance.

(D–E) Volcano plots showing differential gene expression in DR.

(F) Locus-specific visualization of CTSH-associated variants.

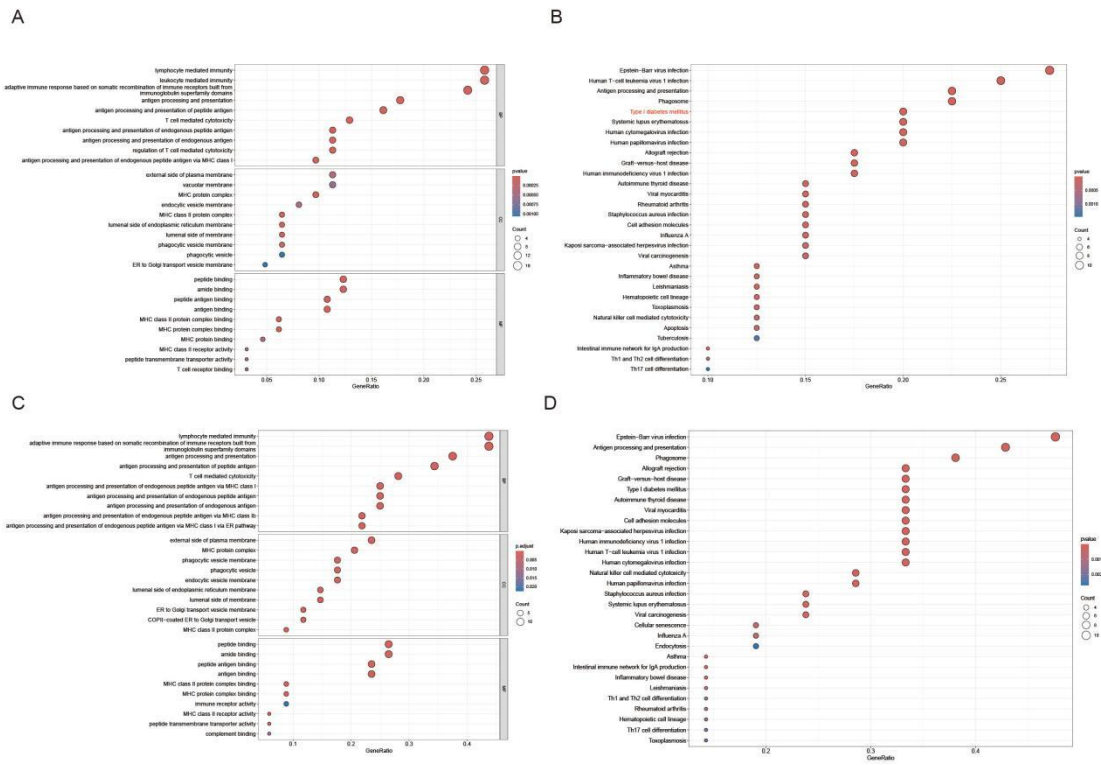


Figure S2. Functional enrichment analyses of CTSH-associated genes

(A–C) Gene ontology (GO) enrichment for immune and antigen presentation pathways.

(B–D) KEGG pathway enrichment highlighting inflammatory and autoimmune signaling.

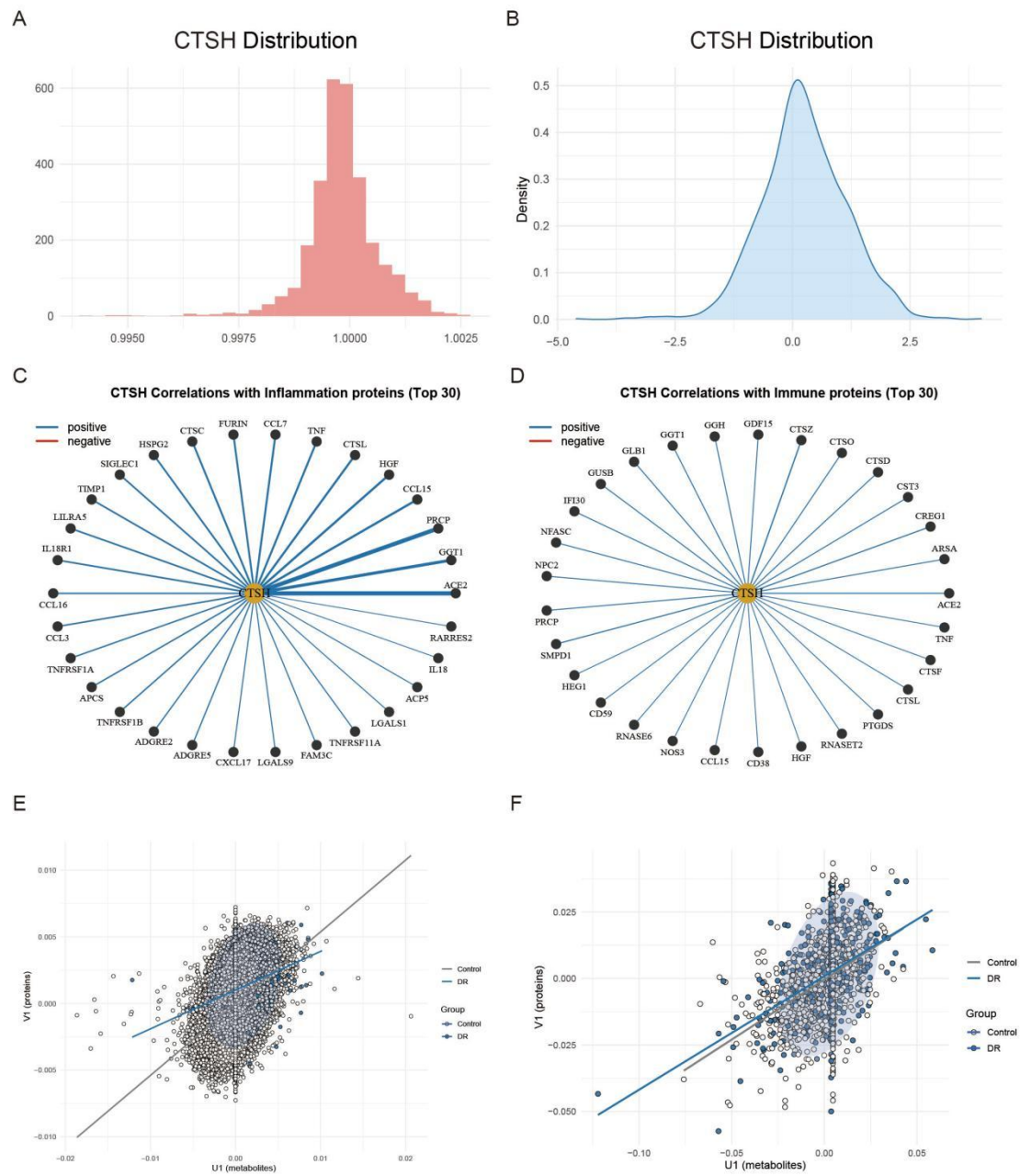


Figure S4. Distribution and correlation patterns of CTSH

(A–B) Distribution density of CTSH levels.

(C–D) Correlation networks between CTSH and inflammatory/immune proteins.

(E–F) Joint metabolite–protein association scatter plots.

Figure S5

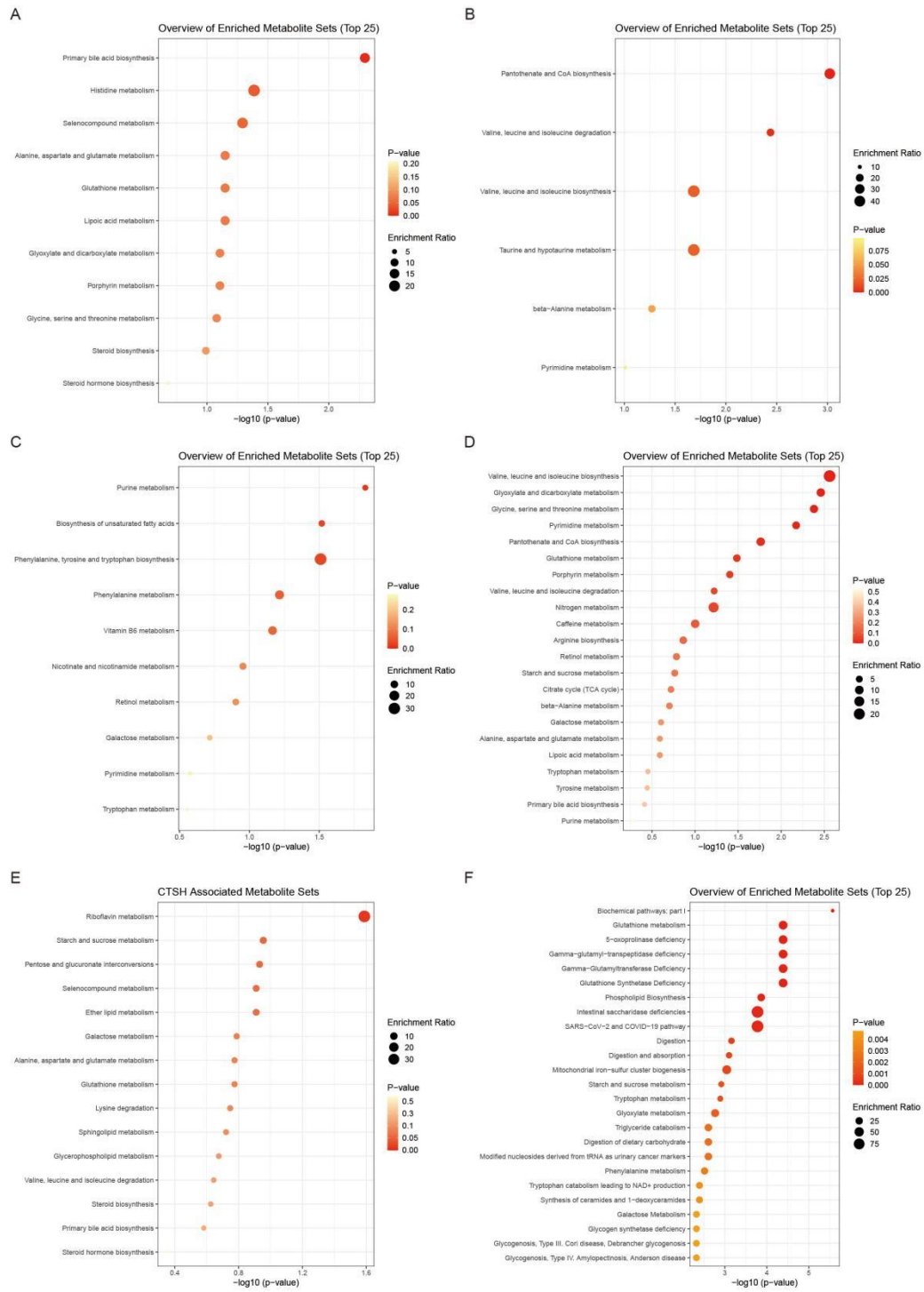


Figure S5. Metabolite enrichment analyses associated with CTSH

(A–D) Overview of enriched metabolite sets.

(E) CTSH-associated metabolic pathways.

(F) Expanded pathway enrichment overview.

Figure S6

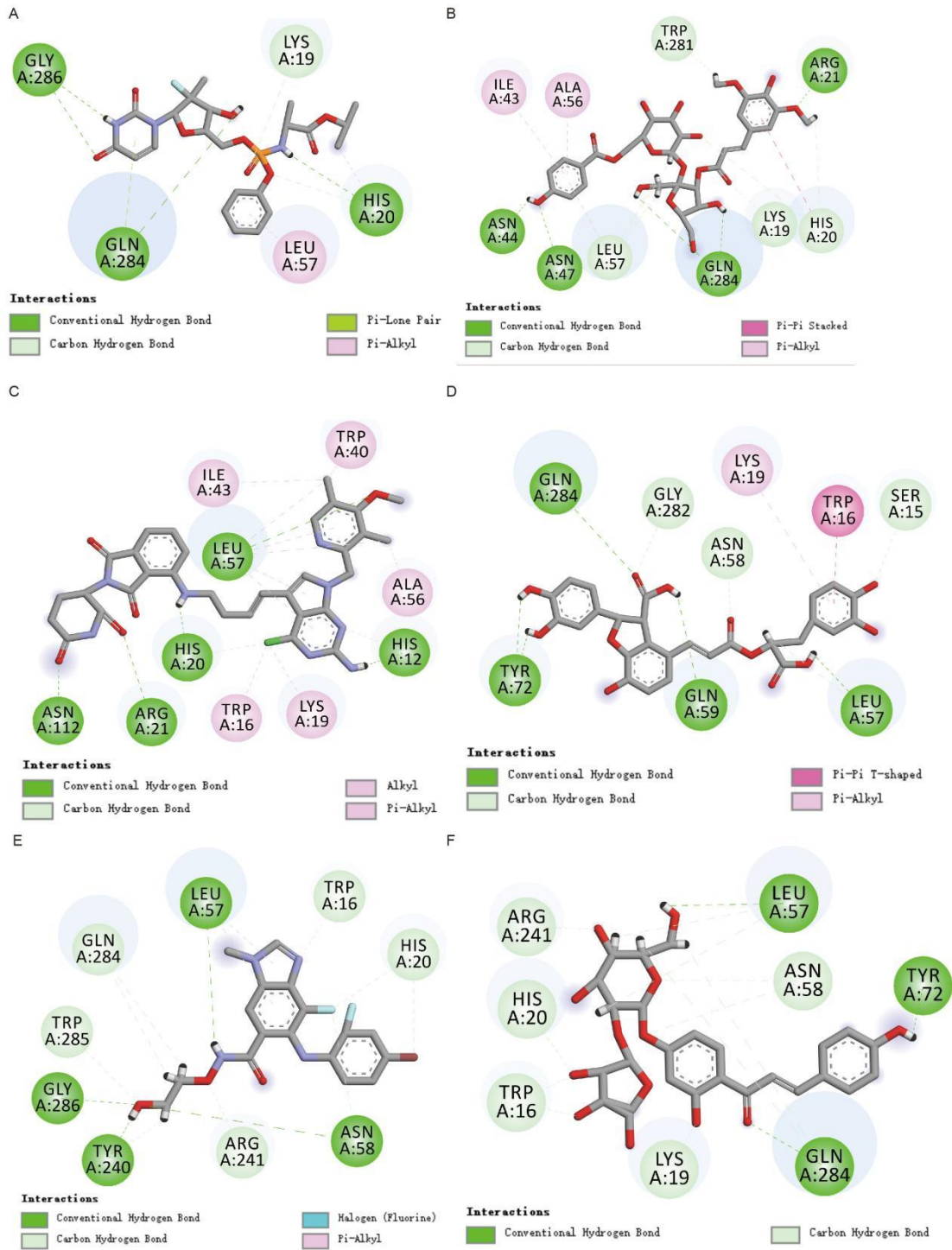


Figure S6. Molecular docking interaction maps

(A–F) Two-dimensional interaction maps of top-ranked CTSH-binding compounds showing hydrogen bonding and hydrophobic interactions.

Figure S7

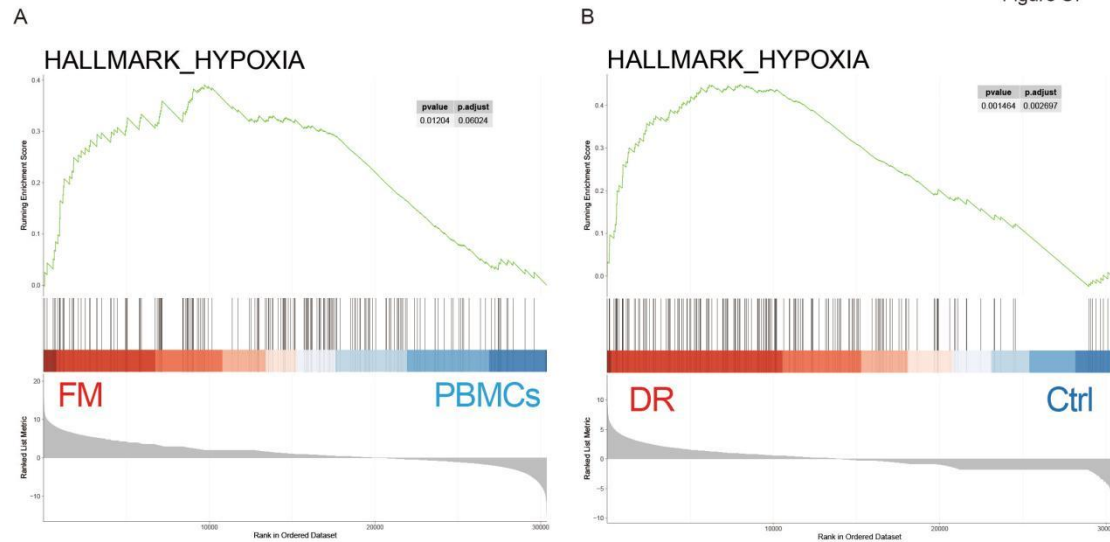


Figure S7. GSEA analysis of hypoxia signatures

(A–B) HALLMARK_HYPOXIA enrichment comparing fibrovascular membranes vs PBMCs and DR vs control.

Figure S8

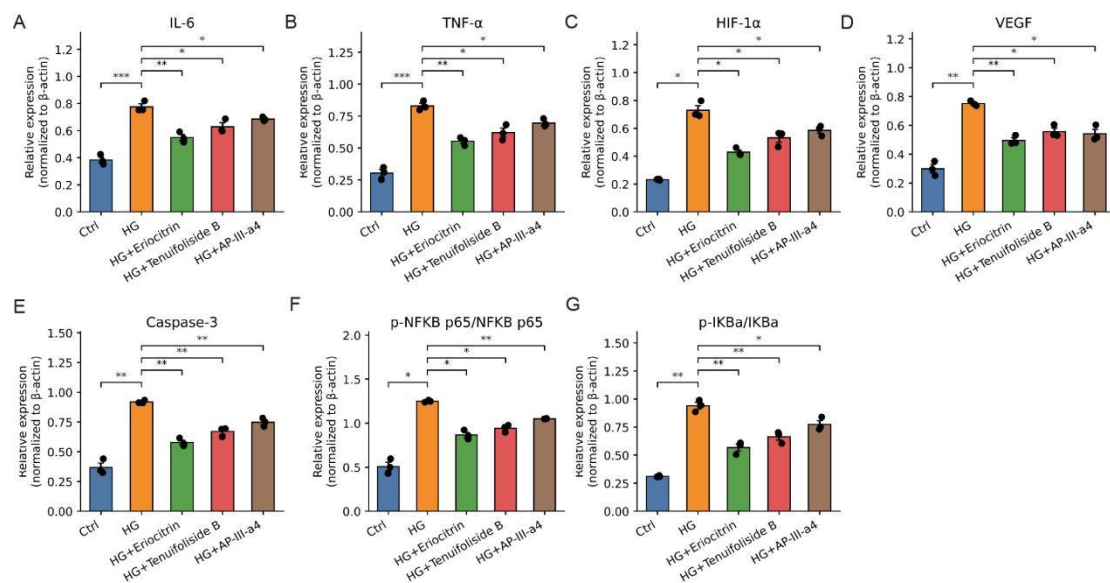


Figure S8. In vitro evaluation of CTSH-targeting compounds

(A–D) Effects of Eriocitrin, Tenuifolside B, and AP-III-a4 on IL-6, TNF- α , HIF-1 α , and VEGF expression under high glucose.

(E–G) Caspase-3, NF- κ B p65, and p-I κ B α /I κ B α ratios.

Figure S9

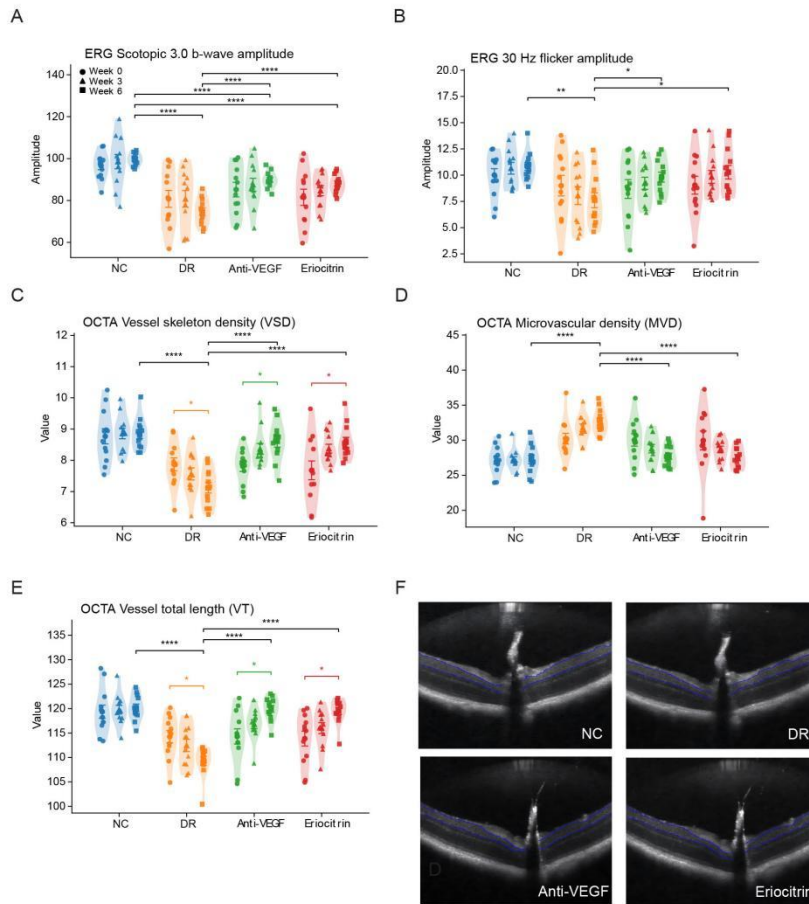


Figure S9. Additional in vivo functional and vascular measurements

(A) Scotopic 3.0 b-wave amplitude.

(B) 30-Hz flicker amplitude.

(C–E) Vessel skeleton density, microvascular density, and vessel total length.

(F) Representative OCT structural images.